

*Regular paper*

## **A comparison of the three isoforms of the light-harvesting complex II using transient absorption and time-resolved fluorescence measurements**

Miguel A. Palacios<sup>1,4,\*</sup>, Joerg Standfuss<sup>3</sup>, Mikas Vengris<sup>1</sup>, Bart F. van Oort<sup>2</sup>, Ivo H.M. van Stokkum<sup>1</sup>, Werner Kühlbrandt<sup>3</sup>, Herbert van Amerongen<sup>2</sup> & Rienk van Grondelle<sup>1</sup>  
<sup>1</sup>*Department of Biophysics and Physics of Complex Systems, Division of Physics and Astronomy, Faculty of Sciences, Vrije Universiteit, De Boelelaan, 1081, 1081 HV Amsterdam, The Netherlands;* <sup>2</sup>*Laboratory of Biophysics, Wageningen Universiteit, Dreijenlaan 3, 6703 HA Wageningen, The Netherlands;* <sup>3</sup>*Department of Structural Biology, Max Planck Institute of Biophysics, D-60439 Frankfurt am Main, 60439 Hessen, Germany;* <sup>4</sup>*Philips Research Laboratories, Care & Health Applications, High Tech Campus 34, Building WB 7.023, Post Box 7.071, 5656 AE Eindhoven, The Netherlands;* \**Author for correspondence (e-mail: miguel.palacios@philips.com; fax: +31-40-27-44288)*

Received 31 August 2005; accepted in revised form 10 January 2006/Published online: 12 May 2006

*Key words:* chlorophyll *a*, chlorophyll *b*, energy transfer, excitonic interactions, light-harvesting complex 2

### **Abstract**

In this article we report the characterization of the energy transfer process in the reconstituted isoforms of the plant light-harvesting complex II. Homotrimers of recombinant Lhcb1 and Lhcb2 and monomers of Lhcb3 were compared to native trimeric complexes. We used low-intensity femtosecond transient absorption (TA) and time-resolved fluorescence measurements at 77 K and at room temperature, respectively, to excite the complexes selectively in the chlorophyll *b* absorption band at 650 nm with 80 fs pulses and on the high-energy side of the chlorophyll *a* absorption band at 662 nm with 180 fs pulses. The subsequent kinetics was probed at 30–35 different wavelengths in the region from 635 to 700 nm. The rate constants for energy transfer were very similar, indicating that structurally the three isoforms are highly homologous and that probably none of them play a more significant role in light-harvesting and energy transfer. No signature has been found in the transient absorption measurements at 77 K for Lhcb3 which might suggest that this protein acts as a relative energy sink of the excitations in heterotrimers of Lhcb1/Lhcb2/Lhcb3. Minor differences in the amplitudes of some of the rate constants and in the absorption and fluorescence properties of some pigments were observed, which are ascribed to slight variations in the environment surrounding some of the chromophores depending on the isoform. The decay of the fluorescence was also similar for the three isoforms and multi-exponential, characterized by two major components in the ns regime and a minor one in the ps regime. In agreement with previous transient absorption measurements on native LHC II complexes, Chl *b* → Chl *a* energy transfer exhibited very fast channels but at the same time a slow component (ps). The Chls absorbing at around 660 nm exhibited both fast energy transfer which we ascribe to transfer from ‘red’ Chl *b* towards ‘red’ Chl *a* and slow transfer from ‘blue’ Chl *a* towards ‘red’ Chl *a*. The results are discussed in the context of the new available atomic models for LHC II.

*Abbreviations:* Chl – chlorophyll; ESA – excited state absorption; fwhm – full width at half maximum; LD – linear dichroism; LHC II – light-harvesting complex II; OD – optical density; PB – photobleaching; PS II – Photosystem II; EADS – evolution associated difference spectra; SE – stimulated emission; TA – transient absorption; v/v – volume per volume; w/v – weight per volume

## Introduction

The major light-harvesting complex of higher plants (LHC II) is the most abundant protein in the thylakoid membrane of the chloroplast. It is mainly associated with Photosystem II (PS II) and functions as an efficient light collector for the reaction center, where excitations lead to charge separation (van Amerongen and Dekker 2003; van Grondelle et al. 1994). Over the past few years a deeper knowledge about its function has been obtained, namely: (i) the absorption of sunlight energy and the efficient transfer to the core of PS II (van Amerongen and Dekker 2003; van Grondelle et al. 1994), (ii) the participation in the regulation of the light-energy distribution between Photosystems I and II in plants (Allen et al. 1981), (iii) the participation in the dissipation of excess excitation energy (Jennings et al. 1991) and (iv) the stacking of the grana (Ke 2001). Because LHC II is a mixture of several isoforms referred to as proteins, Lhcb1, Lhcb2, and Lhcb3, one might wonder whether every individual protein component of LHC II has associated a unique functional property to it, which is strongly suggested by the fact that there are more similarities between the same isoforms belonging to distinct species than between two isoforms of the same plant species (Jansson 1994; Standfuss and Kühlbrandt 2004). The exact proportion/abundance of these proteins in LHC II appears to be variable and species dependent.

Very recently, Standfuss and Kühlbrandt (2004) and Caffarri et al. (2004) concluded that Lhcb1 and Lhcb2 participate in the light-energy distribution between the two photosystems of plants, whereas no clear indication was found to conclude that Lhcb3 participates directly in this process. Additionally, there is some evidence that Lhcb2 becomes phosphorylated three times more rapidly than Lhcb1 (Islam 1987; Jansson and Gustafsson 1990) and therefore, the main role of Lhcb2 seems to be in the adaptation of photosynthesis to different light conditions, both on the short and the long time scale. A lower affinity for neoxanthin binding in Lhcb3 compared to Lhcb1 and Lhcb2 led Caffarri et al. to conclude that Lhcb3 might be a preferential site of regulation of the antenna function in excess light conditions.

The (polarized) absorption and fluorescence spectra of the three isoforms showed that spectra of Lhcb3 exhibited a slight red shift in the location of the maximum in the Chl *a*  $Q_y$  region compared to those of Lhcb1 and Lhcb2 (Standfuss and Kühlbrandt 2004; Caffarri et al. 2004). Furthermore, it was argued that the location of Lhcb3 is the closest to the PS II reaction center of the three isoforms (Standfuss and Kühlbrandt 2004). Therefore, Caffarri et al. (2004) and Standfuss and Kühlbrandt (2004) concluded that Lhcb3 might act as an intermediary of the excitation energy transfer in heterotrimers of Lhcb1/Lhcb2/Lhcb3 and the PS II core.

From a structural point of view all three are highly homologous. All chlorophyll and putative xanthophyll binding sites are conserved, although Lhcb3 might bind 1 Chl *b* molecule less according to Standfuss and Kühlbrandt (2004). However, Caffarri et al. did not report significant differences in the Chl *b* content of the three isoforms. In addition, there is also some discrepancy in the reported Chl *a/b* ratio for the three reconstituted isoforms, which is closer to the value of 1.33 observed in the new crystal structures of LHC II (Liu et al. 2004; Standfuss et al. 2005) in the samples prepared by Caffarri et al. The protein residues which are needed for trimerization of LHC II complexes (Hobe et al. 1995) are conserved in all the isoforms, but in contrast to Lhcb1 and Lhcb2, Lhcb3 alone does not form stable homotrimers *in vitro* (Standfuss and Kühlbrandt 2004; Caffarri et al. 2004). Furthermore, the N terminus of Lhcb3 is 10 residues shorter and lacks the phosphorylation site.

The absorption, fluorescence and circular dichroism spectra of the isoforms are quite similar but, as mentioned above, spectra of Lhcb3 exhibited a slight red shift in the location of the maximum of the red-most band in all spectra as compared to those of Lhcb1 and Lhcb2. Small differences at around 660 nm are observed in the absorption spectra reported by Standfuss and Kühlbrandt and Caffarri et al. The former observe an enhanced absorption cross-section around this wavelength, which might be due to an additional red-shifted Chl *b* absorption subband (the Chl *a/b* ratio was lower in the former preparations, see above). Somewhat larger differences between the isoforms were observed in the LD spectra at 77 K

reported by Caffarri et al. A chlorophyll *a* molecule absorbing at around 676 nm in Lhcb1 showed a different orientation than when bound to Lhcb2 and Lhcb3 (Caffarri et al. 2004). In addition, a Chl *a* in Lhcb1 seems to be replaced by a Chl *b* in Lhcb2, which has been ascribed to a different affinity for Chl *a* or Chl *b* depending on the isoform for that particular binding site. A common characteristic of the isoforms, independent of the procedure followed in the reconstitution is that Lhcb2 at 77 K shows the broadest (fwhm) fluorescence spectrum of the three. However, whereas in the spectra reported by Caffarri et al. Lhcb1 exhibits more fluorescence than Lhcb2 and Lhcb3 at wavelengths between 685 and 700 nm, that is not the case in the spectra reported by Standfuss and Kühlbrandt, where Lhcb2 appears to be the one fluorescing more at those wavelengths. Time-resolved fluorescence measurements have only been reported for reconstituted Lhcb1 and for native LHC II complexes (Ide et al. 1987; Bittner et al. 1994; Connelly et al. 1997; Vasilév et al. 1997; Barzda et al. 2001; Moya et al. 2001; Palacios et al. 2002). Whereas for the former complexes two components were reported (Moya et al. 2001), for the latter a single component or two have been found (Ide et al. 1987; Bittner et al. 1994; Connelly et al. 1997; Vasilév et al. 1997; Barzda et al. 2001; Palacios et al. 2002).

Regarding energy transfer, it has been well established for native LHC II complexes that most of the excitation energy on the Chl *b* molecules is transferred to the Chl *a* molecules with subpicosecond time constants ( $\sim 150$ – $300$  and  $\sim 600$  fs) and only a minor fraction is transferred with a time constant of a few picoseconds (4–9 ps) (Bittner et al. 1994, 1995; Du et al. 1994; Connelly et al. 1997; Kleima et al. 1997; Agarwal et al. 2000; Salverda et al. 2003). For Chl *a*  $\rightarrow$  Chl *a* energy transfer slow components have been found upon blue site excitation, i.e. at around 660 nm (Kwa et al. 1992; Visser et al. 1996, 1997; Gradinaru et al. 1998), but at the same time an ultrafast process has been reported, although it was not unambiguously ascribed to Chl  $\rightarrow$  Chl energy transfer due to the long pulses used in the experiments (200–250 fs) (Visser et al. 1996; Gradinaru et al. 1998). Recently, Croce et al. (2001) performed a detailed transient absorption (TA) study on one of the reconstituted isoforms of LHC II, namely Lhcb1. They reported for both carotenoid

to chlorophyll and chlorophyll to chlorophyll similar transfer times and efficiencies to those of native LHC II complexes. Modeling of the energy-transfer dynamics in LHC II has also been attempted in the past few years (Renger and May, 1997; Gradinaru et al. 1998; Valkunas et al. 1999; Iseri and Gülen 2001; Novoderezhkin et al. 2003). An improvement in the description of the observed rate constants was achieved with a modified Redfield approach, including a strong electron–phonon coupling. Despite the good description of the absorbance, linear dichroism (LD), fluorescence and TA experiments, it should be realized that most of the experimental data were modeled with the atomic model at 3.4 Å resolution obtained by Kühlbrandt et al. (1994). However, very recently new atomic models for LHC II were obtained at 2.72 Å resolution by Liu et al. (2004) and at 2.5 Å by Standfuss et al. (2005) and many of the spectroscopic properties could be satisfactorily modeled (Novoderezhkin et al. 2005). The new model shows two additional chlorophylls and furthermore, the identity and orientation of all the chlorophylls (8 Chls *a* and 6 Chls *b*) were revealed.

For a deeper insight into the functional role of the three isoforms and a better understanding of the energy-transfer dynamics in this system, we examined the light-harvesting and energy-transfer process in the three isoforms by performing TA and time-resolved fluorescence experiments on each of them and compared the result to native LHC II. Selective excitation at 650 nm (8–9 nm, fwhm) and at 662 nm (5–6 nm, fwhm), allowed us to accurately resolve most of the relevant kinetics. Regarding the rate constants, all samples showed similar kinetics, but the reconstituted samples exhibited an enhanced pump-probe signal at around 660 nm, which correlates with the increase in steady-state absorption near this wavelength. The multi-exponential fluorescence decay was similar for all three isoforms.

## Materials and methods

### *Sample preparation*

Native trimeric LHC II was purified from spinach (Peterman et al. 1995) using anion-exchange chromatography and the detergent *n*-dodecyl- $\beta$ -D-

maltoside (Sigma) for solubilization of the complexes. Samples were diluted in a medium containing 20 mM Hepes buffer at pH 7.8 and 0.03% (w/v) *n*-dodecyl- $\beta$ -D-maltoside, whereas the medium for the Lhcb1, Lhcb2 and Lhcb3 isoforms of LHC II contained 40 mM Hepes buffer at pH 7.8 and 0.05% (w/v) *n*-dodecyl- $\beta$ -D-maltoside. In addition, 62% (v/v) of glycerol was added for measurements at 77 K (Oxford cryostat, DN1704). The OD of the samples at the Chl *a*  $Q_y$  maximum measured in a 1-mm-pathlength cuvette ranged from 0.4 to 0.6.

The three recombinant LHC II isoforms were refolded from inclusion bodies and pigments as described previously (Standfuss and Kühlbrandt 2004). To increase the amount of refolded protein the procedure was scaled up to 60 mg inclusion bodies, 50 mg Chl (*a/b* = 3.0) and 15 mg of carotenoids were used in each experiment.

Table 1 shows the pigment stoichiometry, determined by HPLC, of samples prepared identically to the ones used in our study.

#### *Transient-absorption (TA) measurements*

Femtosecond laser pulses were obtained from a titanium:sapphire laser oscillator-regenerative amplifier combination (Coherent MIRA seed and RegA 9050) operated at a repetition rate of 125 kHz, which provided initial 60 fs pulses at 800 nm (fwhm 30 nm). The output was split into two beams: one was focused into a sapphire plate to generate a white-light continuum to be used as the probe pulse. The other beam pumped an infrared optical parametric amplifier (OPA 9850,

Coherent). The output of the OPA was tuned to 1300 and 1324 nm and the frequency doubled to 650 and 662 nm, respectively. The resulting pulse had a bandwidth (fwhm) of 19 nm and a duration of 35 fs. To achieve higher selectivity upon excitation, interference filters with maximum transmittance at 650 and 662 nm were placed after doubling of the 1300 and 1324 nm beams from the OPA. The resulting pulses showed a duration of 80 and 180 fs and a bandwidth of 8–9 and 5–6 nm (fwhm), respectively. The instrument response function of the system, was 85 fs for excitation at 650 nm and 210 fs for 662 nm excitation, estimated from the fwhm of the cross-correlation signal measured after mixing pump and probe beams in a BBO crystal at the place of the sample. Figure 1a shows the cross-correlation signal measured for the case of 650 nm excitation. In all measurements, the polarization of the pump laser beam was set at magic angle (54.7°) with respect to the probe beam by means of a Berek polarization compensator (New Focus, 5540). Individual transient absorption traces were recorded by lock-in detection (EG&G Model 5210) with the pump beam chopped at a frequency of  $f = 612$  Hz. The detection wavelength was selected by focusing the white light probe beam into a monochromator placed after the sample with a bandwidth of 1.5 nm. Thirty to thirty-five traces were collected for every sample in the wavelength range 635–700 nm.

The pump-beam diameter was  $\sim 180$   $\mu\text{m}$  in the focus, determined as fwhm of a Gaussian intensity profile. Excitation intensity used for the measurements was 0.64 nJ/pulse. Under our experimental conditions we estimate that at most, in the worst case, one out of 310 Chl *b* or one out of 140 Chl *a*

Table 1. Pigment stoichiometry<sup>a</sup> (pigment molecules per monomer), determined by HPLC, of samples prepared identically to the ones used in our study

	LHC II	Lhcb1	Lhcb2	Lhcb3
Lutein	1.82 $\pm$ 0.20	2.0	2.0	2.0
Neoxanthin	0.91 $\pm$ 0.16	0.86 $\pm$ 0.02	0.80 $\pm$ 0.08	0.72 $\pm$ 0.05
Violaxanthin	0.21 $\pm$ 0.03	0.07 $\pm$ 0.01	0.07 $\pm$ 0.01	0.14 $\pm$ 0.01
Chl <i>a</i>	8.28 $\pm$ 0.30	8.49 $\pm$ 0.24	8.48 $\pm$ 0.28	8.32 $\pm$ 0.26
Chl <i>b</i>	6.0	7.72 $\pm$ 0.15	7.58 $\pm$ 0.28	6.13 $\pm$ 0.28
Chl <i>a/b</i>	1.38	1.10	1.12	1.36

<sup>a</sup> In the case of native LHC II the amount of chlorophyll *b* was set to 6 per monomer, and the other pigments were scaled to this. For the reconstituted Lhcb1, Lhcb2 and Lhcb3, the amount of lutein was set to 2 per monomer and the other pigments scaled to this. For more details see (Peterman et al. 1997; Standfuss and Kühlbrandt 2004). The values are averages  $\pm$  standard deviations of four (reconstituted Lhcb1, Lhcb2 and Lhcb3) and five independent experiments (native LHC II).

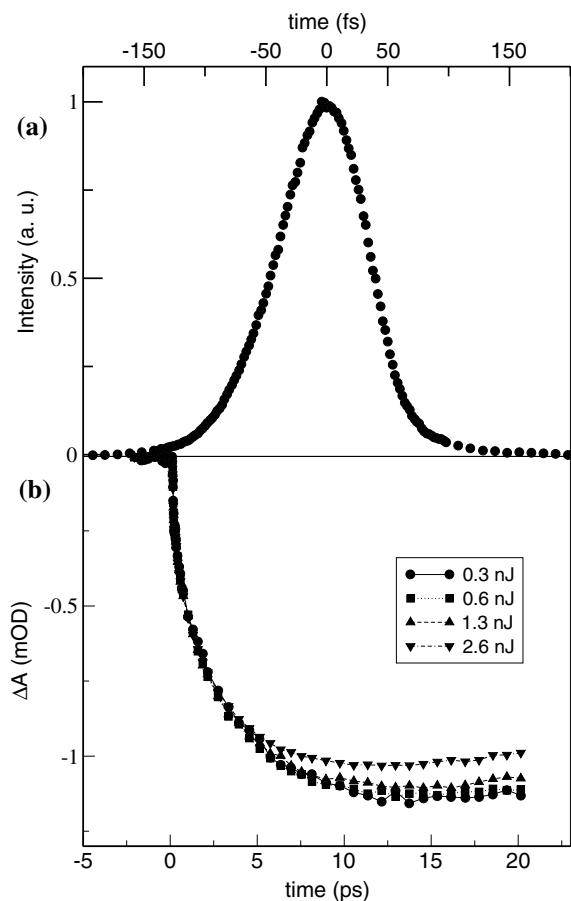


Figure 1. (a) Cross-correlation signal of the pump and probe laser pulses. Excitation wavelength of the pump pulse was 650 nm. (b) Power dependence of the pump-probe signal measured at 679 nm upon 650 nm excitation for homotrimers of Lhcb1. The traces were rescaled by a factor  $1/P$ , where  $P$  is the power used for excitation.

molecules is excited per pulse. Therefore, any annihilation effect is absent in the presented results. These estimates agree with the linear dependence of the transient absorption signal measured at 679 nm as a function of the power intensity between 0.3 and 1 nJ. At higher excitation intensities, the shape of the trace starts to deviate somewhat, reflecting the loss of excitations (see Figure 1b for homotrimers of Lhcb1).

#### Time-resolved fluorescence measurements

Time-resolved fluorescence was recorded with time-correlated single-photon counting. Briefly, 0.2 ps pulses (430 nm, 3.8 MHz) were produced

by a mode-locked titanium:sapphire laser (Coherent Inc., Mira 900-D), with pulse picker, frequency doubler and Glan-laser polarizer. Fluorescence was collected at  $54.7^\circ$  through a rotatable sheet type polarizer and a 665 nm long-pass filter. Individual photons were detected by a micro-channel plate photomultiplier (PMT, Hamamatsu R3809U-50). Single photon responses of the PMT were amplified by a wide-band amplifier (Becker & Hickl GmbH, Berlin, Germany), analyzed by a constant fraction discriminator (CFD, Tennelec Inc. Oak Ridge, TS) and stored in a multi-channel analyzer (4096 channels). With a small portion of the mode-locked light at 860 nm a fast PIN-photodiode was excited. The output pulses of this photodiode were analyzed by another channel of the CFD, and then used as stop signal for the TAC. The channel spacing was 0.5 ps. The excitation intensity was reduced with neutral density filters to obtain a count-rate below 30,000 per second (Vos et al. 1987) and care was taken to minimize data distortion (van Hoek and Visser 1985). The samples were kept at  $20^\circ\text{C}$ . The instrument response function (50 ps, fwhm) was obtained from pinacyanol chloride in methanol, which has a fluorescence lifetime of 10 ps. Home-written software was used for data analysis (Novikov et al. 1999; Digris et al. 1999).

#### Data analysis

Pump-probe data were analyzed using a global fitting routine as described previously (van Stokkum et al. 2004). Datasets for the same excitation wavelength were fit together in an irreversible sequential model with 4 (662 nm excitation) or 5 (650 nm excitation) lifetimes, yielding evolution-associated difference spectra (EADS) and their corresponding lifetimes. This procedure enabled us to visualize the evolution of the excited states in the system. The final EADS represents the equilibrated excited state, i.e. when all the energy transfer processes are completed, which lives longer than the measuring time window (20 ps). The fwhm of the instrument response function in the data analysis, fit with a Gaussian profile, agreed with the bandwidth obtained from the experimentally measured cross-correlation signal and deviations were at most  $\pm 10$  fs.

## Results

### *Absorption, LD spectra and time-resolved fluorescence*

The absorption, second derivative and LD spectra at 77 K of native complexes and of the three isoforms, Lhcb1, Lhcb2 and Lhcb3, are shown in Figure 2. Absorption spectra are similar in shape and peak positions to the absorption spectra of the three isoforms reported by Standfuss and Kühlbrandt (2004), but they differ from those of Caffarri et al. (2004) mostly around 660 nm. This might be due to the presence of an additional red-shifted Chl *b* absorption subband (Standfuss and Kühlbrandt reported a lower Chl *a/b* ratio than Caffarri et al.). In addition, the absorption spectrum of all the isoforms shows an enhanced absorption cross-section in the Chl *b*  $Q_y$  and in the high-energy side of the Chl *a* absorption region, when compared to that of native trimers. Probably, a Chl *a* experiences a different environment and/or a Chl *a* is replaced by a Chl *b*, inducing the loss of Chl *a* absorption around 676 nm and the appearance of absorption around 660 nm. A red shift in the main Chl *b* absorption band is observed in the absorption spectrum of Lhcb3, in agreement with previous results (Standfuss and Kühlbrandt 2004; Caffarri et al. 2004). Our Lhcb3 preparation seems to bind somewhat less Chl *b* than Lhcb1 and Lhcb2 (a factor of 0.14 times less) when comparing integrated areas at 640–660 nm after normalization of the Chl *a* absorption intensity at 660–710 nm.

The positions of all the absorption subbands (see Figure 2b) are very close to those of the native complexes, both monomers and trimers (see also Hemelrijk et al. 1992; Nussberger et al. 1994; van Amerongen et al. 1994; Ruban et al. 1997; Palacios et al. 2003), and are very similar for the different isoforms, suggesting a similar pigment organization in the complexes. Only small shifts are observed.

In the LD spectra of the complexes, the maximum of the red-most band due to Chl *a* is located at 676.5 (LHC II), 678 (Lhcb1), 676 (Lhcb2) and 679 nm (Lhcb3). A shoulder at around 662 nm is observed for all the complexes, in correspondence with the absorption spectra, although the intensity varies depending on the isoform. From the spectra it is clear that some Chl *b* molecules in Lhcb1

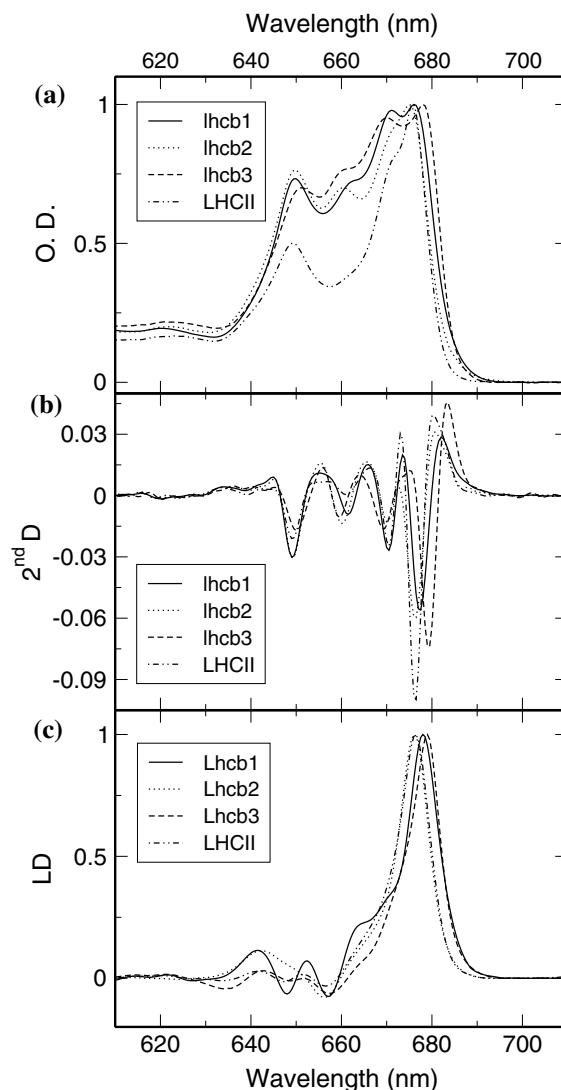


Figure 2. (a) Normalized absorption spectra at 77 K of native LHC II trimers, homotrimers of Lhcb1 and Lhcb2 and monomers of Lhcb3. (b) Second derivative of the absorption spectra. (c) Linear dichroism spectra at 77 K of native LHC II trimers, homotrimers of Lhcb1 and Lhcb2 and monomers of Lhcb3.

might be oriented differently than in Lhcb2 (here we compare only homotrimers of Lhcb1 with homotrimers of Lhcb2 and not with monomers of Lhcb3), as the signal at wavelength around 650 nm is somewhat different for both complexes. The comparison of our  $\Delta A$  and  $\Delta LD$  for Lhcb1 minus Lhcb2 does not clearly indicate that a Chl *a* in Lhcb1 is replaced by a Chl *b* in our preparations (results not shown), in contrast to the results of Caffarri et al. In line with their results, it seems that a Chl *a* absorbing at around 676 nm in our

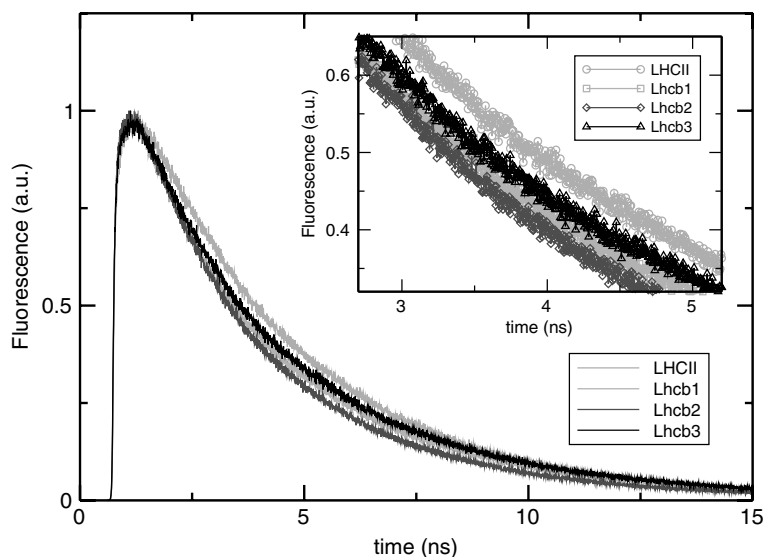
Lhcb1 preparation changes its orientation to some extent in Lhcb2. Note that the LD spectra, which depend critically on overall and mutual orientations of pigments, are very similar, showing that for (nearly) all the pigments the organization is the same in all preparations.

Figure 3 shows time-resolved fluorescence decay traces measured at room temperature for native complexes and the three isoforms of LHC II – Lhcb1, Lhcb2 and Lhcb3 – after excitation at 430 nm. The decay of the fluorescence turned out to be similar in all complexes and was multi-exponential. The time constants derived from a fit of the decay traces are shown in Table 2. It can be seen that all complexes exhibit two components in the ns regime and only the reconstituted complexes show a minor component in the ps regime. This minor component accounts for less than 10% of the decay in the isoforms. The three isoforms exhibit similar time-constants and amplitudes, but the amplitudes of the ns components differed from those of native LHC II. Whereas in native complexes the longest ns component had an amplitude of  $\sim 0.9$ , in the reconstituted complexes it had an amplitude of 0.5–0.6.

#### *Chl b* $\rightarrow$ *Chl a* energy transfer

Excitation of the complexes with 650 nm centered pulses leads to fast (fs) and slow (ps) energy

transfer from the Chl *b* to the Chl *a* molecules, which absorb at lower energy. This is illustrated by the kinetic traces collected at several probe wavelengths for Lhcb3 monomers in Figure 4. The first plot reflects the decay in the Chl *b* absorption region. To visualize the energy transfer processes, a linear scale between  $-0.2$  and  $0.6$  ps and a logarithmic scale between  $0.6$  and  $20$  ps has been chosen. It can be observed that some Chl *b* molecules exhibit fast subpicosecond energy transfer processes, but at the same time slow picosecond components are present, implying that at least one Chl *b* molecule exhibits slow transfer. The ‘blue’ Chls *b* absorbing at around  $645$  nm exhibit a faster decay than the ‘red’ Chls *b* absorbing at  $655$ – $660$  nm. This feature has recently been reported and modeled for LHC II (Novoderezhkin et al. 2004) (see Discussion). In the second plot (linear scale between  $-0.2$  and  $0.2$  ps and logarithmic from  $0.2$  till  $20$  ps) kinetic traces in the intermediate region between the main Chl *b* and Chl *a* absorption bands are depicted. The kinetic traces in this region are crucial for understanding the energy transfer dynamics in LHC II (Novoderezhkin et al. 2003). As discussed by Novoderezhkin et al. (2004, 2005) they reflect (i) fast population of these intermediate states in the first  $200$  fs, (ii) a competition between somewhat slower population of these states and fast energy transfer towards more red absorbing Chls *a*



*Figure 3.* Time-resolved fluorescence traces at room temperature of native LHC II trimers and homotrimers of Lhcb1 and Lhcb2 and monomers of Lhcb3 after excitation at 430 nm. The fluorescence was collected using a 665 nm long-pass filter. The instrument response function was 50 ps, fwhm. The inset shows the decay between 3 and 5 ps.

Table 2. Fluorescence lifetimes ( $\tau$ ) and their amplitudes ( $p$ ) obtained after a fit of the first 12 ns of the decay of the fluorescence for native LHC II trimers, homotrimers of Lhcb1 and Lhcb2 and monomers of Lhcb3

LHC II		Lhcb1		Lhcb2		Lhcb3	
$\tau$ (ns)	$p$						
–	–	0.20	0.13	0.18	0.10	0.22	0.08
1.51	0.09	1.73	0.34	1.64	0.35	1.85	0.34
3.77	0.91	4.22	0.53	3.77	0.55	4.32	0.58

(region between 0.1 and  $\sim 1$  ps) giving rise to the nonmonotonic features observed at around 200 fs and (iii) final picosecond energy transfer reflected by the loss of signal. The third plot shows a rapid increase of the signal in the red part of the absorption spectrum, which corresponds with the rapid decrease of the signal observed at around 650 nm and final equilibration among the Chls *a*. This final equilibration process can be seen in the decay of the signal for kinetic traces between 670 and 676 nm and slow population of the states absorbing above 676 nm (note that in the third plot the whole scale is linear in time).

In order to compare the energy transfer process between all the isoforms and native LHC II complexes and to obtain the energy transfer time constants, a global analysis fit of the pump-probe data was performed. The EADS obtained from a sequential model for 650 nm excitation are shown in Figure 5. Due to the high similarity in all cases, we will describe only the Lhcb2 isoform and highlight the small differences that exist with the results for the other complexes. The first EADS represents the exciton population created at time zero by the laser pulse. The Chl *a* molecules become partly excited via the vibronic wing of the  $Q_y$  transition. The first EADS is replaced by the second EADS in 130 fs and the amplitude at 650 nm of the latter is half of the former, which implies that half of the excitations flow from Chl *b* towards Chl *a* with a time constant of about 130 fs, in agreement with previous TA measurements on monomers and trimers of LHC II at 77 K (Bittner et al. 1995; Kleima et al. 1997). The lowest energy states which absorb at around 680 nm (Pieper et al. 1999) receive the excitation energy very fast, as can be deduced from the rapid rise of its bleaching/stimulated emission (PB/SE) in the first couple of hundreds of femtoseconds. Intermediate states located between 660 and

675 nm become populated too, in correspondence with the qualitative description of the kinetic traces (see above and Figure 4). Compared to native complexes, these intriguing intermediate states show an enhanced pump-probe signal for these reconstituted complexes. With a time constant of 0.62 ps the second EADS evolves into the third EADS, reflecting energy transfer from Chl *b* to Chl *a* and from intermediate states absorbing at 660–670 nm, towards Chls absorbing lower in energy (670–680 nm). The third EADS has a lifetime of 2.9 ps which reflects some slow transfer from the intermediate states towards the lowest energy state(s) but, at the same time, slow Chl *b*  $\rightarrow$  Chl *a* energy transfer, as can be deduced from the loss of amplitude at 650 nm. When the fourth EADS appears, the bleaching at around 660 nm is masked by excited state absorption (ESA), leading to a positive signal in this wavelength region. Final equilibration of the excitation in the Chl *a* region is observed in the last two EADS, which shows up in the spectra as a red shift of the minimum located at around 675–680 nm. This final equilibration process seems to be less pronounced for the Lhcb3 complexes, where a shift towards the red is not clearly observed.

The Lhcb3 EADS are the narrowest, whereas the EADS obtained for Lhcb2 complexes are the broadest. This is in agreement with the absorption spectra (see Figure 2a) where, for instance, the main Chl *b* absorption band for Lhcb2 peaking at 650 nm is broader than that of Lhcb1 and Lhcb3 and with the steady-state fluorescence spectra of Caffarri et al. and Standfuss and Kühlbrandt, whose fluorescence spectrum at 77 K of Lhcb2 is the broadest (fwhm) of the three isoforms. The obtained energy transfer time constants for all the isoforms of LHC II and native complexes are very similar (see also Table 3) and in agreement with previously reported rate constants for wild-type

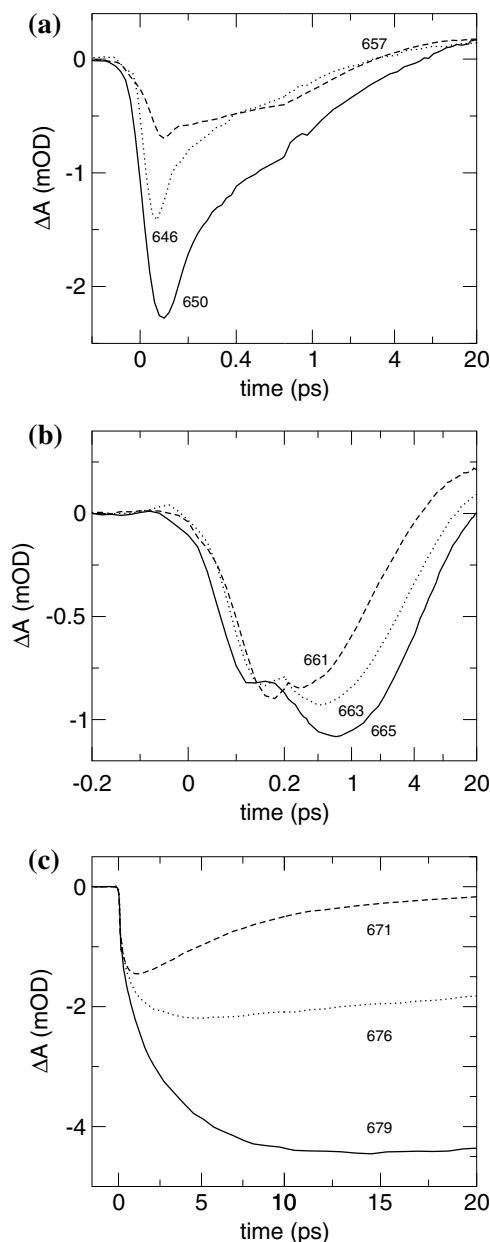


**Figure 4.** Kinetic traces for monomers of Lhcb3 upon 650 nm excitation. Note that in (a) the scale is linear between  $-0.2$  and  $0.6$  ps, whereas it is logarithmic between  $0.6$  and  $20$  ps. In (b), it is linear between  $-0.2$  and  $0.2$  ps and logarithmic from  $0.2$  till  $20$  ps. In C the whole scale is linear.

LHC II complexes (see for instance, Kwa et al. 1992; Bittner et al. 1994, 1995; Du et al. 1994; Visser et al. 1996, 1997; Connelly et al. 1997; Kleima et al. 1997; Gradinaru et al. 1998; Agarwal et al. 2000). Overall, it is important to note that the pump-probe data of the complexes studied,

which depend critically on mutual orientations of pigments, are virtually identical, showing that for (nearly) all the pigments the organization is the same in all preparations.

#### *Chl a $\rightarrow$ Chl a energy transfer*

The energy transfer processes from ‘blue’ absorbing Chls *a* at around  $660$ – $670$  nm, towards the lowest energy states in the LHC II complexes, have proven to be crucial in understanding the energy-transfer dynamics in LHC II (Novoderezhjin et al. 2003). Slow components in the ps regime have previously been reported by Gradinaru et al. (1998) ( $5$  ps for LHC II monomers), Visser et al. (1996) ( $2.4$  ps for trimers), and Kwa et al. (1992) ( $3$  ps for trimers). To selectively excite these states, the  $662$  nm excitation laser pulse was  $5$ – $6$  nm broad (fwhm) with a pulse length of  $180$  fs. Again, the results for one of the isoforms, Lhcb1 in this case, will be described and the differences with the other isoforms highlighted.

Figure 6a shows the sequential model for Lhcb1 homotrimers after global analysis of the TA data. The first EADS shows that almost no population is created on the Chls *b* which absorb at  $650$  nm or higher in energy. The minimum of the first EADS is located at  $661.5$  nm and the fwhm of the PB/SE signal is  $9.5$  nm. Like for  $650$  nm excitation, the Chl *a* molecules absorbing at  $675$ – $680$  nm become partly excited via their vibronic bands. Whereas in the three isoforms the signal at  $661$  nm is larger than at  $675$ – $680$  nm at time zero, the situation is reversed for native complexes, where a larger signal at  $675$ – $680$  nm is observed, probably due to the lower absorption cross-section at  $\sim 660$  nm in native complexes compared to the reconstituted isoforms. The first EADS decays with a time constant of  $\sim 500$  fs, implying that one or more states around  $655$ – $665$  nm transfer their excitation(s) relatively fast. These states have recently been ascribed to ‘red’ Chls *b* (Novoderezhjin et al. 2004). The lifetime of the second EADS is  $2.7$  ps, reflecting energy transfer from ‘blue’ to ‘red’ Chl *a*. This process dominates the evolution of the excited states upon  $662$  nm excitation. The final equilibration process occurs with a time constant of about  $17$  ps and the positive signal due to ESA at  $660$ – $670$  nm appears. Again, the equilibration process above  $670$  nm is less pronounced for

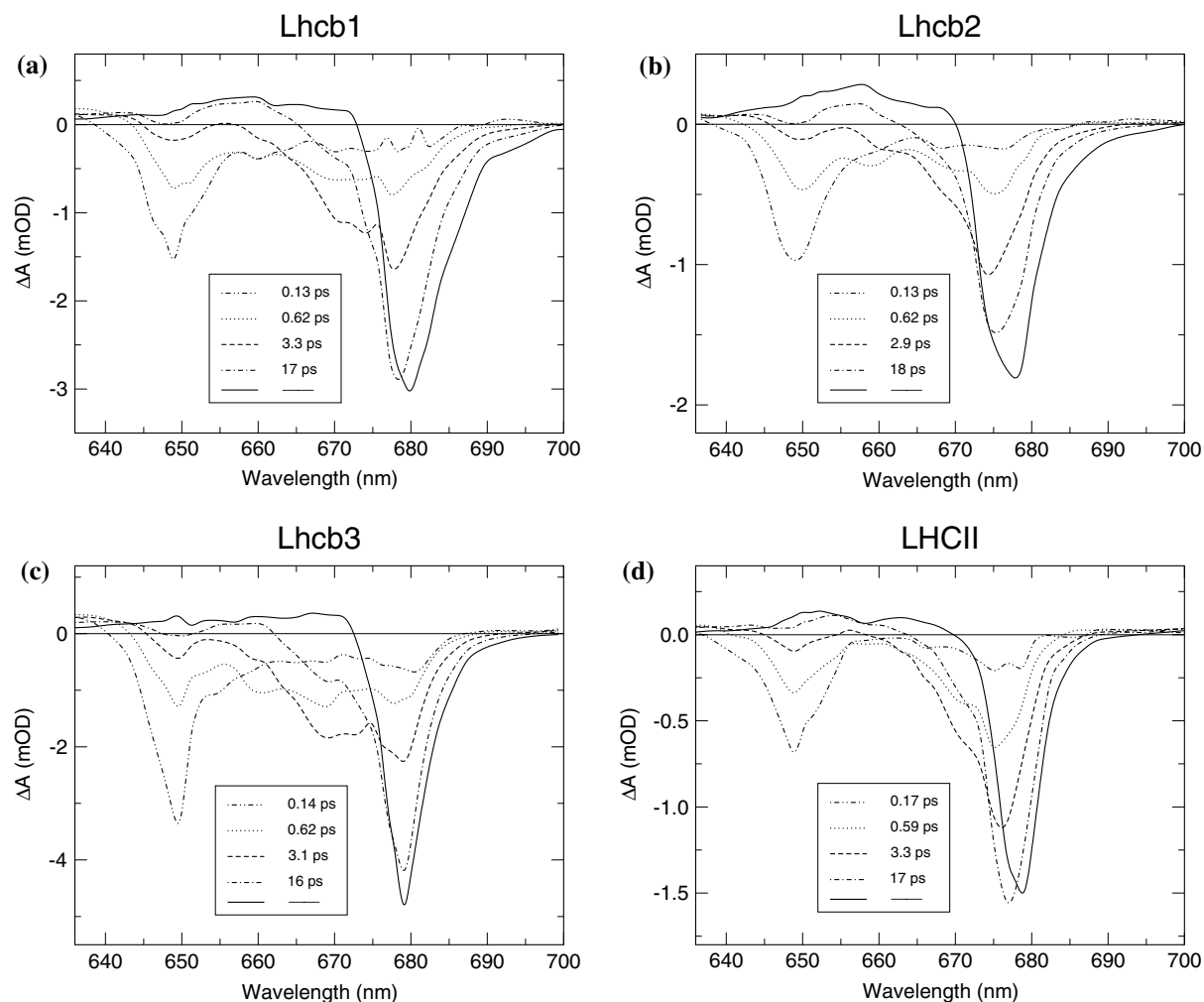


Figure 5. EADS obtained with a sequential model for homotrimers of Lhcb1 (a), homotrimers of Lhcb2 (b), monomers of Lhcb3 (c) and native complexes (d). Excitation wavelength: 650 nm, pulse duration: 80 fs, fwhm 8–9 nm. The time constants in the legend of every figure represent the lifetime of every EADS, i.e. the first EADS is prepared by the pump beam at  $t=0$  and lives for  $\sim 130$  fs. Subsequently, the second EADS appears and lives for about 600 fs, being replaced by the third EADS, which in turn lives for  $\sim 3$  ps. Finally, after that lifetime the fourth EADS shows up living for 17 ps and being replaced by the fifth EADS.

Lhcb3 complexes than for Lhcb1 and Lhcb2. Like in the case of 650 nm excitation, the energy transfer rates for the three isoforms of LHC II are very similar to those of the native complexes (see Table 3).

## Discussion

### *Fluorescence lifetimes of the isoforms*

The fluorescence decay for the three isoforms is very similar and faster than for native LHC II. Three components were obtained after a fit of the

decay traces for Lhcb1, Lhcb2 and Lhcb3, one in the ps regime and two in the ns regime. For native LHC II complexes only two components (ns) were found (see Table 2). Recently, Moya et al. have correlated the existence of two decay components in the ns regime to the existence of two conformations of the LHC II backbone (Moya et al. 2001). It was suggested that one of them might dissipate excess energy and be correlated with the shortest component, whereas the other conformation, associated with the longest component, would participate in light-harvesting and energy transfer. However, there are also studies in which a single component has been measured (Bittner et al.

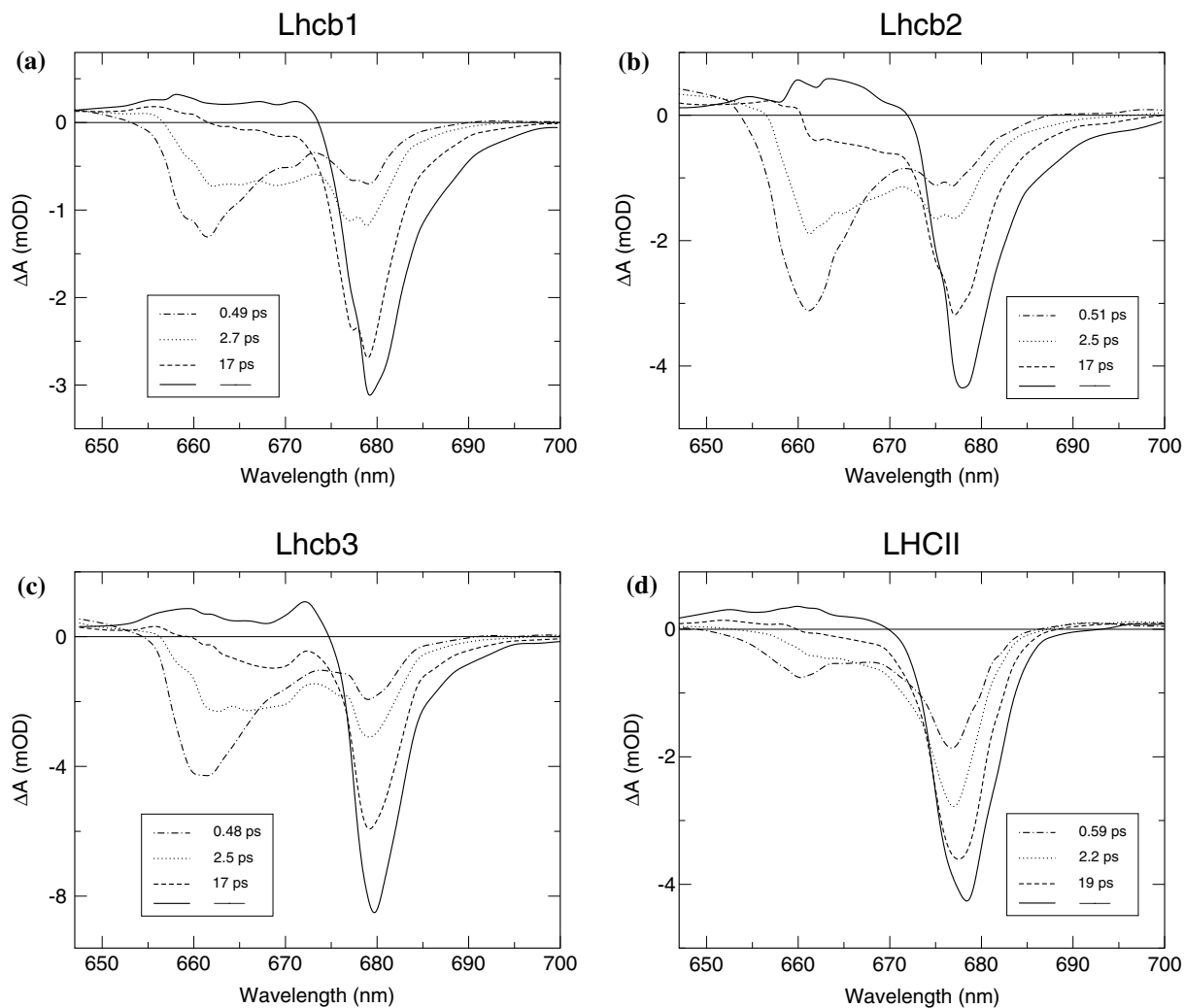


Figure 6. EADS obtained with a sequential model for homotrimers of Lhcb1 (a), homotrimers of Lhcb2 (b), monomers of Lhcb3 (c) and native complexes (d). Excitation wavelength: 662 nm, pulse duration: 180 fs, fwhm 5–6 nm. The time constants in the legend of every figure represent again the lifetime of every EADS (see Figure 5 for a more detailed explanation).

1994; Connelly et al. 1997; Barzda et al. 2001; Palacios et al. 2002). It seems that the number of components depends on sample preparation.

#### Energy transfer

Chl *b* → Chl *a* energy transfer occurs predominantly fast. Upon excitation at 650 nm all isoforms and the native trimers of LHC II exhibit fast energy transfer from the Chl *b* molecules towards the Chls *a*. The ‘blue’ Chl *b* PB/SE disappears more rapidly than the signal of the ‘red’ Chls *b*, reflecting intra-band equilibration within a pair of Chl *b* molecules due to strong coupling of Chl *b* molecules

(Novoderezhjin et al. 2004). In view of the new crystal structures (Liu et al. 2004; Standfuss et al. 2005), this may only occur between the Chls 10 and 13, which form the pair of Chls *b* that exhibit the strongest coupling strength. The lowest energy state(s) absorbing at around 680 nm (Pieper et al. 1999) become(s) populated during the first few hundreds of fs. This suggests some exciton delocalization and relatively strong interactions between one or two pairs of chlorophylls *a* and *b*, as pointed out very recently by Novoderezhkin et al. (2004) and by Leupold et al. (2002). Only a minor fraction (~10%) of the Chl *b* excitations is transferred to Chls *a* on a picosecond regime. This

Table 3. Energy transfer time constants (ps) obtained after a global fit of the transient absorption data with a sequential model

Sample	650 nm <sup>a</sup>				662 nm <sup>b</sup>		
	$t_1$	$t_2$	$t_3$	$t_4$	$t_1$	$t_2$	$t_3$
Lhcb1	0.13	0.62	3.3	17	0.49	2.7	17
Lhcb2	0.13	0.62	2.9	18	0.51	2.5	17
Lhcb3	0.14	0.62	3.1	16	0.48	2.5	17
Native	0.17	0.59	3.3	17	0.59	2.2	19

<sup>a</sup> The laser pulse was centered at 650 nm, 8–9 nm broad (fwhm) and had a duration of 80 fs.

<sup>b</sup> The laser pulse was centered at 662, 5–6 nm broad (fwhm) and had a duration of 180 fs.

Deviations in the given numbers are estimated to be  $\pm 10\%$ .

is in qualitative agreement with the new atomic models of LHC II, where all Chl *b* molecules with the exception of Chl *b* 14 are close to a Chl *a* and transfer rates faster than  $(1 \text{ ps})^{-1}$  can be expected. Slow (ps) Chl *b*  $\rightarrow$  Chl *a* energy transfer has also been reported for native complexes in the literature (Bittner et al. 1994, 1995; Visser et al. 1996; Connelly et al. 1997; Kleima et al. 1997). The obtained transfer times for Chl *b*  $\rightarrow$  Chl *a* transfer in Lhcb1 (see Table 2) are somewhat different from those obtained by Croce et al. (2001). They reported transfer times of 0.13, 0.33, 1 and 7 ps. This discrepancy might be due to the approach followed to fit the experimental data and/or the different excitation conditions (Croce et al. did not perform selective excitation of the Chls *b* at 77 K, but rather of the xanthophylls bound to LHC II at 277 K).

Although the energy transfer rate constants are very similar for all the complexes (see Table 3), some small differences on the energy transfer process between the isoforms do occur. For instance, the amplitude of the fastest component, i.e. that of about 130 fs, is larger for Lhcb3 monomers than for Lhcb1 and Lhcb2 homotrimers. This can be seen in Figure 7, where the fit at  $\sim 655$  nm for all the complexes is shown. Whereas for the former the ratio of the amplitudes between the 130 and the 600 fs components is 2:1, for the latter complexes it is 1:1. This implies that in Lhcb3, the fast processes show a larger contribution than for Lhcb1 and Lhcb2. On the other hand, the fit of the kinetics at  $\sim 672$  nm depicted in Figure 7 shows that the final equilibration process in the Chl *a* band taking about 17 ps, possesses a larger contribution in Lhcb2 than in Lhcb1 and Lhcb3 at that particular wavelength. Finally, in Figure 7 it can be observed that LHC II native

trimers exhibit properties close to the average of all three isoforms. This can be appreciated in the contribution of every component to the fit of both kinetics (655 and 672 nm).

Chl *a*  $\rightarrow$  Chl *a* energy transfer upon blue side excitation is slow. Excitation of ‘blue’ Chls *a* leads to substantially slower transfer than Chl *b* excitation. The instrument response function of the setup for the 662 nm excitation experiment was 210 fs, which would impede the detection of processes significantly faster than 200 fs. However, previous studies on native LHC II did not report faster rates upon 660 nm excitation (Kwa et al. 1992; Gradinaru et al. 1998; Visser et al. 1996, 1997). The fastest decay time that we observe is  $\sim 0.5$  ps. It has been concluded that this step should be ascribed to transfer from ‘red’ Chls *b* absorbing mainly between 655 and 660 nm (Novoderezhkin et al. 2004). The second EADS is red-shifted with respect to the first EADS, indicating that the ‘red’ Chls *b* transfer excitations more rapidly than the ‘blue’ Chls *a*. Like for the Chl *b*  $\rightarrow$  Chl *a* energy transfer case, bleaching signals at 670 and 675 nm appear in the evolution of the EADS, implying that many pathways exist for the energy flow before excitations reach the lowest energy state (see (Novoderezhkin et al. 2004) for a rather detailed description).

The ‘blue’ Chls *a* transfer excited state energy towards the lowest energy state(s) relatively slowly with a time constant of 2.5 ps (disappearance of the initial bleaching signal at wavelengths between 660 and 670 nm upon going from the second to the third EADS in Figure 6). A similar transfer time was reported by Gradinaru et al. (1998), Visser et al. (1996, 1997), and Kwa et al. (1992). Final equilibration within the Chl *a* pool is achieved again in about 17 ps. This slow equilibration has

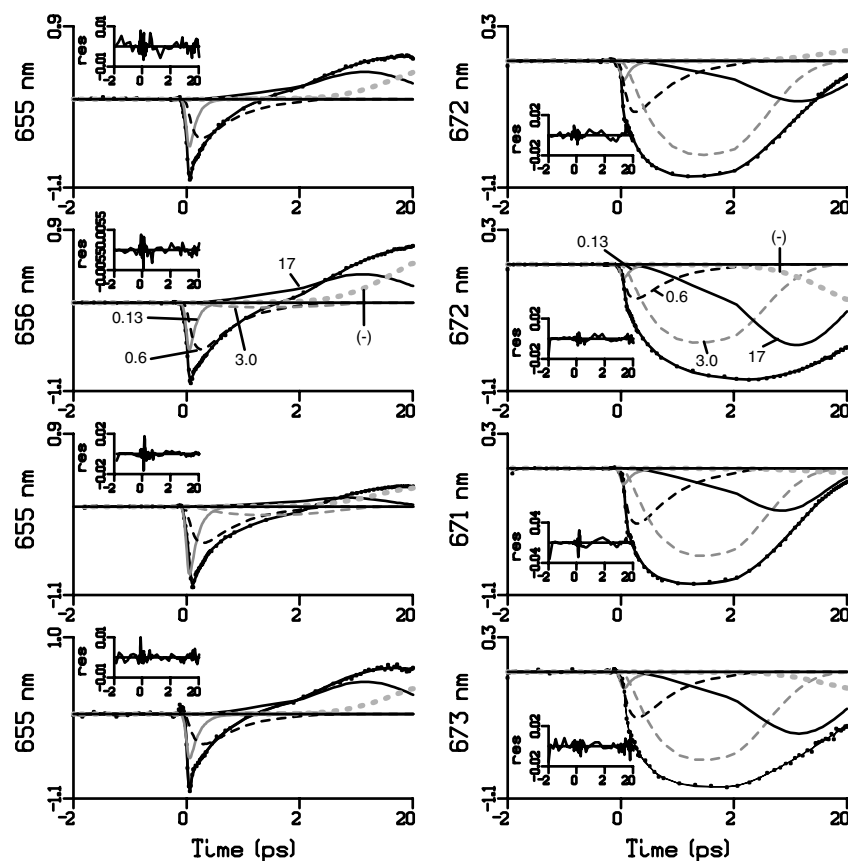


*Figure 7.* Fit of normalized kinetic traces upon 650 nm excitation at 77 K of the three isoforms Lhcb1, Lhcb2 and Lhcb3 and of native LHC II complexes. Probe wavelengths are  $\sim 655$  nm and  $\sim 672$  nm. Points are experimental data, continuous black line over the points is the fit of the kinetics. The contribution of every component to the fit is shown in solid grey (0.13 ps), dashed black (0.6 ps), dashed light grey (3.0 ps), solid black (17 ps) and dotted light grey (component associated to the decay of the final excited states and which lives longer than the experimental time window). The contribution of two ‘compensating’ ultrafast components (1–2 fs) needed to fit a coherent artifact present at other wavelengths has been omitted for the clarity of the figure. The residuals from the fit are shown in the insets. Note that the time scale is linear from  $-2$  to 2 ps and logarithmic thereafter.

been ascribed to energy transfer from Chls *a* located at the luminal to Chls *a* in the stromal side (Novoderezhkin et al. 2004, van Amerongen and van Grondelle 2001). All the reconstituted samples exhibited an enhanced pump-probe signal between 655 and 665 nm (see Figures 5 and 6) compared to native complexes, which we ascribe to the larger absorption cross-section at those wavelengths observed in the steady-state absorption spectra of the reconstituted isoforms. The ESA observed in this wavelength region after equilibration appears to be an intrinsic property of the LHC II complexes (see also, Visser et al. 1996; Gradinaru et al. 1998), and it probably arises from excitonic interactions (Buck et al. 1997; Amerongen et al. 2000).

#### *Towards a physiological role for Lhcb1, Lhcb2 and Lhcb3*

In order to get a deeper insight into the light-harvesting and energy-transfer function of the three isoforms of LHC II, we investigated transient absorption (TA) and time-resolved fluorescence measurements on reconstituted homotrimers of Lhcb1 and Lhcb2 and monomers of Lhcb3. The overall energy-transfer process seems to be very similar in all the isoforms and energy transfer rate constants are identical within experimental error. Therefore, it can be concluded that small variations in the environment surrounding the chromophores may tune the absorption and fluorescence wavelengths of the pigments slightly, but

this does not lead to significant differences in the energy-transfer function of the three isoforms. These results are in line with fluorescence excitation measurements reported by Caffarri et al. (2004), who did not find any difference in Chl  $b \rightarrow$  Chl  $a$  and carotenoid  $\rightarrow$  Chl transfer efficiency between the isoforms (95 and 80%, respectively). In fact, all the Chl binding sites are conserved and only a change in the orientation of one Chl  $a$  molecule absorbing at around 676 nm, when comparing Lhcb1 to Lhcb2 and Lhcb3, has been reported (Caffarri et al. 2004). However, this does not have a significant effect on the overall energy-transfer kinetics.

The final EADS in all cases reflects the equilibrated excited state. The equilibration time is a factor of 100 shorter than the excited state lifetime(s) or fluorescence lifetime(s) as was shown above. Therefore, essentially all steady-state fluorescence arises from the state that corresponds to the final EADS. Its location and fwhm is somewhat different in the three isoforms of LHC II, which implies that the absorption wavelength associated to the lowest energy states may vary between isoforms. This might explain why Pieper et al. (1999) were able to burn three different holes in solubilized trimers of LHC II at 4.2 K in the red edge of the absorption spectrum. Figure 8 shows the normalized final EADS for the three isoforms after excitation at 662 nm and Table 4 shows the location and fwhm of the final EADS for all three of them. It can be seen that, for instance, Lhcb2 exhibits a blue-shifted final EADS compared to Lhcb1 and Lhcb3 and it turns out to be the broadest of all three as well, in agreement with previous steady-state fluorescence data (Standfuss and Kühlbrandt, 2004; Caffarri et al. 2004). Furthermore, the steady-state (polarized) absorption and fluorescence data show that the location of the maximum in Lhcb3 is slightly red shifted compared to those of Lhcb1 and Lhcb2, which is also observed in our final EADS. It is much narrower than that of Lhcb1, which agrees with the fluorescence data at 77 K reported by Caffarri et al. In line with their results, the final EADS associated to Lhcb1 shows more PB/SE at longer wavelengths than those of Lhcb2 and Lhcb3 at low temperatures. However, Standfuss and Kühlbrandt (2004) reported that Lhcb2 showed more fluorescence at longer wavelengths than Lhcb1 and Lhcb3.

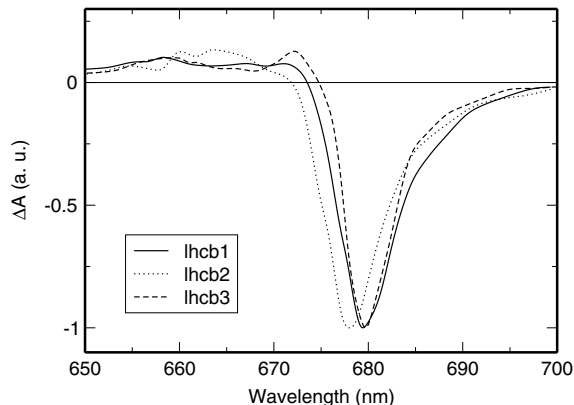


Figure 8. Normalized final EADS for Lhcb1, Lhcb2 and Lhcb3 at 77 K after selective excitation at 662 nm.

Table 4. Location of the minimum  $\lambda$  and fwhm of the final EADS for homotrimers of Lhcb1 and Lhcb2 and monomers of Lhcb3

Lhcb1		Lhcb2		Lhcb3	
$\lambda$ (nm)	fwhm (nm)	$\lambda$ (nm)	fwhm (nm)	$\lambda$ (nm)	fwhm (nm)
679.4	7.1	678.1	7.2	679.7	5.7

Excitation wavelength: 662 nm.

The energy differences between the emitting states of Lhcb1, Lhcb2 and Lhcb3 are much smaller than the Boltzmann factor  $k_B T$ , which corresponds to approximately 10 nm in this wavelength region at room temperature. Therefore, the probability to find an excitation on either Lhcb1, Lhcb2 or Lhcb3 is hardly dependent on the differences in spectral composition, but almost entirely on the relative occurrence of these proteins in the thylakoid membrane. Given the fact that Lhcb3 is far less present than Lhcb1 and Lhcb2, it cannot function as a thermodynamic energy sink, as was speculated before based on similar reconstituted Lhcb proteins.

Standfuss and Kühlbrandt argued that the location of Lhcb3 is the closest to the PS II core of those of Lhcb1, Lhcb2 and Lhcb3 (Standfuss and Kühlbrandt 2004). In that case, Lhcb3 might be an intermediary in the excitation energy transfer, but our results do not show a spectroscopic feature to suggest such a role. Recently, Caffarri et al. (2004) hypothesized that Lhcb3 might be a preferential site of regulation of the antenna function in excess

light conditions. Evidently, the role of Lhcb3 still remains to be determined, but it is clear that its spectroscopic and light-harvesting properties are nearly identical to those of Lhcb1 and Lhcb2. In contrast to Lhcb3, knowledge about the main functional properties associated to Lhcb1 and Lhcb2 is more extensive. Lhcb1 and Lhcb2 possess a phosphorylation site and therefore, both proteins would be able to participate alone in the light-energy distribution between photosystem I and II (Standfuss and Kühlbrandt 2004; Caffarri et al. 2004). Evidence that Lhcb2 becomes phosphorylated three times faster than Lhcb1 (Islam et al. 1987; Jansson and Gustafsson 1990) led Standfuss and Kühlbrandt (2004) to the conclusion that the main role of Lhcb2 might be in the adaptation of photosynthesis to different light conditions.

## Conclusions

Chl *b* → Chl *a* energy transfer exhibits very fast channels, the fastest ones corresponding to time constants of only ~130 and ~600 fs. Only a minor fraction of the excitations on the Chls *b* is transferred with a time constant of a few picoseconds.

'Blue' absorbing Chls *b* show a faster decay of the initial bleaching signal than the 'red' Chls *b* (see Figure 4), which may be due to intraband equilibration within a Chl *b* dimer (see also, Novoderezhkin et al. 2004, 2005).

Selective excitation at 662 nm leads mainly to slow processes (~2.5 ps) due to 'blue' Chls *a* → 'red' Chls *a* energy transfer, but at the same time to fast (~500 fs) energy transfer which we ascribe to 'red' Chls *b* → Chl *a* energy transfer. The final spectral equilibration within the Chl *a* pool occurs with a time constant of 17 ps at 77 K.

Time-resolved fluorescence measurements did not show any significant difference between the three isoforms, which all exhibit a multi-exponential decay characterized by three components. The two shortest components might be correlated with a dissipative conformation of the protein backbone, as suggested before (Moya et al. 2001).

Lhcb1, Lhcb2 and Lhcb3 exhibit similar Chl → Chl energy transfer rates and efficiencies (Caffarri et al. 2004) and therefore, all three most probably play a similar role in light-harvesting and energy transfer in photosynthesis.

Spectroscopically there is no evidence that Lhcb3 acts as relative energy sink of the excitations or as energetic intermediary of the excitation energy transfer in heterotrimers of Lhcb1/Lhcb2/Lhcb3.

## Acknowledgements

Part of the work was supported by the 'Stichting voor Fundamenteel Onderzoek der Materie (FOM)', which is financially supported by the 'Nederlandse Organisatie voor Wetenschappelijk Onderzoek (NWO)'.

## References

- Agarwal R, Krueger BP, Scholes GD, Yang M, Yom J, Mets L and Fleming GR (2000) Ultrafast energy transfer in LHC-II revealed by three-pulse photon echo peak shift measurements. *J Phys Chem B* 104: 2908–2918
- Allen JF, Bennett J, Steinback KE and Arntzen CJ (1981) Chloroplast protein phosphorylation couples plastoquinone redox state to distribution of excitation energy between photosystems. *Nature* 291: 25–29
- Barzda V, Gulbinas V, Kananavicius R, Cervinskas V, van Amerongen H, van Grondelle R and Valkunas L (2001) Singlet-singlet annihilation kinetics in aggregates and trimers of LHC II. *Biophys J* 80: 2409–2421
- Bittner T, Irrgang KD, Renger G and Wasielewski MR (1994) Ultrafast excitation energy transfer and exciton-exciton annihilation processes in isolated light-harvesting complexes of Photosystem II (LHC II) from spinach. *J Phys Chem* 98: 11821–11826
- Bittner T, Wiederrecht GP, Irrgang KD, Renger G and Wasielewski MR (1995) Femtosecond transient absorption spectroscopy on the light-harvesting Chl *a/b* protein complex of Photosystem II at room temperature and 12 K. *Chem Phys* 194: 311–322
- Buck DR, Savikhin S and Struve W (1997) Ultrafast absorption difference spectra of the Fenna-Matthews-Olson protein at 19 K: Experiment and simulations. *Biophys J* 72: 24–36
- Caffarri S, Croce R, Cattivelli L and Bassi R (2004) A look within LHC II: Differential analysis of the Lhb1–3 complexes building the major trimeric antenna complex of higher-plant photosynthesis. *Biochemistry* 43: 9467–9476
- Connelly JP, Müller MG, Hucke M, Gatzgen G, Mullineaux CW, Ruban AV, Horton P and Holzwarth AR (1997) Ultrafast spectroscopy of trimeric light-harvesting complex II from higher plants. *J Phys Chem B* 101: 1902–1909
- Croce R, Müller MG, Bassi R and Holzwarth AR (2001) Carotenoid-to-chlorophyll energy transfer in reconstituted major light-harvesting complex (LHC II) of higher plants. I. Femtosecond transient absorption measurements. *Biophys J* 80: 901–915
- Digris AV, Skakum VV, Novikov EG, van Hoek A and Visser AJWG (1999) Thermal stability of a flavoprotein assessed from associative analysis of polarized time-resolved fluorescence spectroscopy. *Eur Biophys J* 28: 526–531

- Du M, Xie X, Mets L and Fleming GR (1994) Direct observation of ultrafast energy-transfer processes in light harvesting complex II. *J Phys Chem* 98: 4736–4741
- Gradinaru CC, Özdemir S, Gülen D, van Stokkum IHM, van Grondelle R and van Amerongen H (1998) The flow of excitation energy in LHC II monomers: Implications for the structural model of the major plant antenna. *Biophys J* 75: 3064–3077
- Hemelrijk PW, Kwa SLS, van Grondelle R and Dekker JP (1992) Spectroscopic properties of LHC-II, the main light-harvesting chlorophyll *a/b* protein complex from chloroplast membranes. *Biochim Biophys Acta* 1098: 159–166
- Hobe S, Foerster R, Klingler J and Paulsen H (1995) N-proximal sequence motif in light-harvesting chlorophyll *a/b* binding protein is essential for the trimerization of light-harvesting chlorophyll *a/b* complex. *Biochemistry* 34: 10224–10228
- Ide JP, Klug DR, Kühlbrandt W, Giorgi LB and Porter G (1987) The state of detergent solubilised light-harvesting chlorophyll-*a/b* protein complex as monitored by picosecond time-resolved fluorescence and circular dichroism. *Biochim Biophys Acta* 893: 349–364
- Iseri EI and Gülen D (2001) Chlorophyll transition dipole moment orientations and pathways for flow of excitation energy among the chlorophylls of the major plant antenna, LHC II. *Eur Biophys J* 30: 344–353
- Islam K (1987) The rate and extent of phosphorylation of the two light-harvesting chlorophyll *a/b* binding protein complex (LHC-II) polypeptides in isolated spinach thylakoids. *Biochim Biophys Acta* 893: 333–341
- Jansson S (1994) The light-harvesting chlorophyll *a/b*-binding proteins. *Biochim Biophys Acta* 1184: 1–19
- Jansson S and Gustafsson P (1990) Type I and Type II genes for the chlorophyll *a/b*-binding protein in the gymnosperm *Pinus sylvestris* (Scots pine): cDNA cloning and sequence analysis. *Plant Mol Biol* 14: 287–296
- Jennings RC, Garlaschi FM and Zucchelli G (1991) Light-induced fluorescence quenching in the light-harvesting chlorophyll *a/b* protein complex. *Photosyn Res* 27: 57–64
- Ke B (2001) Photosynthesis, vol. 10 of *Advances in Photosynthesis*, chap. 12, Kluwer Academic Publishers, Dordrecht
- Kleima FJ, Gradinaru CC, Calkoen F, van Stokkum IHM, van Grondelle R and van Amerongen H (1997) Energy transfer in LHC II monomers at 77 K studied by sub-picosecond transient absorption spectroscopy. *Biochemistry* 36: 15262–15268
- Kühlbrandt W, Wang DN and Fujiyoshi Y (1994) Atomic model of plant light-harvesting complex by electron crystallography. *Nature* 367: 614–621
- Kwa SLS, van Amerongen H, Lin S, Dekker JP, van Grondelle R and Struve WS (1992) Ultrafast energy transfer in LHC-II trimers from the chl *a/b* light-harvesting antenna of Photosystem II. *Biochim Biophys Acta* 1102: 202–212
- Leupold D, Teuchner K, Ehlert J, Irrgang KD, Renger G and Lokstein H (2002) Two-photon excited fluorescence from higher electronic states of chlorophylls in photosynthetic antenna complexes: A new approach to detect strong excitonic chlorophyll *a/b* coupling. *Biophys J* 82: 1580–1585
- Liu Z, Yan H, Wang K, Kuang TJZ, Gui L, An X and Chang W (2004) Crystal structure of spinach major light-harvesting complex at 2.72 Å resolution. *Nature* 428: 287–292
- Moya I, Silvestri M, Vallon O, Cinque G and Bassi R (2001) Time-resolved fluorescence analysis of the Photosystem II antenna proteins in detergent micelles and liposomes. *Biochemistry* 40: 12552–12561
- Novikov EG, van Hoek A, Visser AJWG and Hofstraat JW (1999) Linear algorithms for stretched exponential decay analysis. *Opt Commun* 166: 189–198
- Novoderezhkin V, Palacios MA, van Amerongen H and van Grondelle R (2005) Excitation dynamics in the LHC II complex of higher plants: modeling based on the 2.72 Å crystal structure. *J Phys Chem B* 109: 10493–10504
- Novoderezhkin V, Salverda JM, van Amerongen H and van Grondelle R (2003) Exciton modeling of energy-transfer dynamics in the LHC II complex of higher plants: A redfield theory approach. *J Phys Chem B* 107: 1893–1912
- Novoderezhkin VI, Palacios MA, van Amerongen H and van Grondelle R (2004) Energy-transfer dynamics in the LHC II complex of higher plants: Modified Redfield approach. *J Phys Chem B* 108: 10363–10375
- Nussberger S, Dekker JP, Kühlbrandt W, van Bolhuis BM, van Grondelle R and van Amerongen H (1994) Spectroscopic characterization of three different monomeric forms of the main chlorophyll *a/b* binding protein from chloroplast membranes. *Biochemistry* 33: 14775–14783
- Palacios MA, de Weerd FL, Ihalainen JA, van Grondelle R and van Amerongen H (2002) Superradiance and exciton (de)localization in light-harvesting complex II from green plants. *J Phys Chem B* 106: 5782–5787
- Palacios MA, Frese RN, Gradinaru CC, van Stokkum IHM, Permyrdhan LL, Horton P, Ruban AV, van Grondelle R and van Amerongen H (2003) Stark spectroscopy of the light-harvesting complex II in different oligomerisation state. *Biochim Biophys Acta* 1605: 83–95
- Peterman EJG, Dukker FM, van Grondelle R and van Amerongen H (1995) Chlorophyll *a* and carotenoid triplet states in light-harvesting complex II of higher plants. *Biophys J* 69: 2670–2678
- Peterman EJG, Gradinaru CC, Calkoen F, Borst JC, van Grondelle R and van Amerongen H (1997) Xanthophylls in light-harvesting complex II of higher plants: Light harvesting and triplet quenching. *Biochemistry* 36: 12208–12215
- Pieper J, Rätsep M, Jankowiak R, Irrgang KD, Voigt J, Renger G and Small GJ (1999)  $Q_y$ -Level structure and dynamics of solubilized light-harvesting complex II of green plants: Pressure and hole burning studies. *J Phys Chem A* 103: 2412–2421
- Renger T and May V (1997) Theory of multiple exciton effects in the photosynthetic antenna complex LHC-II. *J Phys Chem B* 101: 7232–7240
- Ruban AV, Calkoen F, Kwa SLS, van Grondelle R, Horton P and Dekker JP (1997) Characterisation of LHC II in the aggregated state by linear and circular dichroism spectroscopy. *Biochim Biophys Acta* 1321: 61–70
- Salverda JM, Vengris M, Krueger BP, Scholes GD, Czarnoleski AR, Novoderezhkin V, van Amerongen H and van Grondelle R (2003) Energy transfer in light-harvesting complexes II and CP29 of spinach studied with three pulse echo peak shift and transient grating. *Biophys J* 84: 450–465
- Standfuss J and Kühlbrandt W (2004) The three isoforms of the light-harvesting complex II. *J Biol Chem* 279: 36884–36891
- Standfuss J, van Scheltinga ACT, Lamborghini M and Kühlbrandt W (2005) Mechanisms of photoprotection and non-photochemical quenching in pea light-harvesting complex at 2.5 Å resolution. *EMBO J* 24: 919–928
- Valkunas L, Cervinskis V, Trinkunas G, Müller MG and Holzwarth AR (1999) Effects of excited state mixing on

- transient absorption spectra in dimers: Application to photosynthetic light-harvesting complex II. *J Chem Phys* 111: 3121–3132
- van Amerongen H and Dekker JP (2003) Light-harvesting in Photosystem II. In: Parson WW (ed) *Light-Harvesting Antennas in Photosynthesis*, pp 219–251. Kluwer Academic Publishers, Dordrecht, The Netherlands
- van Amerongen H, Kwa SLS, van Bolhuis BM and van Grondelle R (1994) Polarized fluorescence and absorption of macroscopically aligned light harvesting complex II. *Biophys J* 67: 837–847
- van Amerongen H, Valkunas L and van Grondelle R (2000) *Photosynthetic Excitons* (1st ed.). World Scientific, Singapore
- van Amerongen H and van Grondelle R (2001) Understanding the energy transfer function of LHC II, the major light-harvesting complex of green plants. *J Phys Chem* 105: 604–617
- van Grondelle R, Dekker JP, Gillbro T and Sundström V (1994) Energy transfer and trapping in photosynthesis. *Biochim Biophys Acta* 1187: 1–65
- van Hoek A and Visser AJWG (1985) Artefact and distortion sources in time correlated single photon counting. *Analyt Instrument* 14: 359–378
- van Stokkum IHM, Larsen DS and van Grondelle R (2004) Global and target analysis of time-resolved spectra. *Biochim Biophys Acta* 1657: 82–104
- Vasil'ev S, Irrgang KD, Schrötter T, Bergmann A, Eichler HJ and Renger G (1997) Quenching of chlorophyll *a* fluorescence in the aggregates of LHC II: Steady state fluorescence and picosecond relaxation kinetics. *Biochemistry* 36: 7503–7512
- Visser HM, Kleima FJ, Stokkum IHM, van Grondelle R and van Amerongen H (1996) Probing the many energy-transfer processes in the photosynthetic light-harvesting complex II at 77 K using energy-selective sub-picosecond transient absorption spectroscopy. *Chem Phys* 210: 297–312
- Visser HM, Kleima FJ, Stokkum IHM, van Grondelle R and van Amerongen H (1997) Probing the many energy-transfer processes in the photosynthetic light-harvesting complex II at 77 K using energy-selective sub-picosecond transient absorption spectroscopy. *Chem Phys* 215: 299
- Vos K, van Hoek A and Visser AJWG (1987) Application of a reference deconvolution method to tryptophan fluorescence in proteins. A refined description of rotational dynamics. *Eur J Biochem* 165: 55–63